



Red blood cell coagulation induced by low-temperature plasma treatment[☆]



Kenji Miyamoto^{a, b}, Sanae Ikehara^a, Hikaru Takei^b, Yoshihiro Akimoto^c, Hajime Sakakita^d, Kenji Ishikawa^e, Masashi Ueda^f, Jun-ichiro Ikeda^g, Masahiro Yamagishi^a, Jaeho Kim^d, Takashi Yamaguchi^a, Hayao Nakanishi^h, Tetsuji Shimizuⁱ, Nobuyuki Shimizu^j, Masaru Hori^e, Yuzuru Ikehara^{a, k, *}

^a Biotechnology Research Institute for Drug Discovery, National Institute of Advanced Industrial Science and Technology (AIST), Tsukuba, 305-8568, Japan

^b Medical Business Development Division, Nikon Co., Ltd., Yokohama, 244-8533, Japan

^c Department of Anatomy, Kyorin University School of Medicine, Mitaka, 181-8611, Japan

^d Electronics and Photonics Research Institute, AIST, Tsukuba, 305-8568, Japan

^e Graduate School of Engineering, Nagoya University, Nagoya, 464-8603, Japan

^f Graduate School of Medicine, Dentistry, and Pharmaceutica Science, Okayama University, Okayama, 700-8530, Japan

^g Graduate School of Medicine, Osaka University, Suita, 565-0871, Japan

^h Aichi Cancer Center Hospital, Nagoya, 464-8681, Japan

ⁱ Terraplasma GmbH, 85748, Garching, Germany

^j SANNO Hospital, Akasaka, 107-0052, Japan

^k Graduate School of Medicine, Chiba University, Chiba, 107-0052, Japan

ARTICLE INFO

Article history:

Received 21 January 2016

Received in revised form

11 March 2016

Accepted 24 March 2016

Available online 28 March 2016

Keywords:

Low-temperature plasma

Blood coagulation

Clot

Red blood cells

ABSTRACT

Low-temperature plasma (LTP) treatment promotes blood clot formation by stimulation of the both platelet aggregation and coagulation factors. However, the appearance of a membrane-like structure in clots after the treatment is controversial. Based on our previous report that demonstrated characteristics of the form of coagulation of serum proteins induced by LTP treatment, we sought to determine whether treatment with two plasma instruments, namely BPC-HP1 and PN-110/120TPG, formed clots only from red blood cells (RBCs). LTP treatment with each device formed clots from whole blood, whereas LTP treatment with BPC-HP1 formed clots in phosphate-buffered saline (PBS) containing 2×10^9 /mL RBCs. Light microscopic analysis results showed that hemolysis formed clots consisting of materials with membrane-like structures from both whole blood and PBS-suspended RBCs. Moreover, electron microscopic analysis results showed a monotonous material with high electron density in the formed clots, presenting a membrane-like structure. Hemolysis disappeared with the decrease in the current through the targets contacting with the plasma flare and clot formation ceased. Taken together, our results and those of earlier studies present two types of blood clot formation, namely presence or absence of hemolysis capability depending on the current through the targets.

© 2016 Elsevier Inc. All rights reserved.

1. Introduction

Blood circulation carries components including erythrocytes,

which transport O₂ and collect CO₂; leukocytes, which detect invasion of foreign bodies; thrombocytes, which are responsible for clot formation to stop bleeding; and plasma, which acts as a solvent. Loss of large amounts of these components is life-threatening because of the lack of a central machinery to maintain body homeostasis. Hence, many kinds of technology to achieve hemostasis have been developed and improved. For example, to control surgical site bleeding, numerous clinical and technical advances have been established to control spurting and oozing by clipping and ligation, and using surgical hemostats and energy devices,

[☆] This article is part of a Special Issue entitled Low-temperature Plasma in biology and medicine, edited by Hori Masaru, Eun Ha Choi, and Shinya Toyokuni.

* Corresponding author. Biotechnology Research Institute for Drug Discovery, National Institute of Advanced Industrial Science and Technology (AIST), Tsukuba, 305-8568, Japan.

E-mail address: yuzuru-ikehara@aist.go.jp (Y. Ikehara).

respectively [1–6]. Notably, the energy devices and surgical hemostats [7] have been used for oozing to obtain greater visibility rather than to prevent excessive blood loss by spurting. Their performances have been improved to further minimize their invasiveness in order to reduce the risk of intraoperative and postoperative complications [8].

Use of high-frequency electrical coagulators (HFECs), which cauterizes tissues by using electrical current flowing through stromal tissues to stop bleeding, can cause postoperative complications [8]. The basic mechanism of hemostasis in other energy devices is tissue coagulation, which is the same as that in HFECs. However, the basic mechanism of hemostasis by surgical hemostats is to maintain both platelet aggregation and activation of coagulation cascades that are targets for anti-coagulation therapy [9]. From the viewpoint of minimal invasiveness, the use of surgical hemostats has recently increased in order to decrease the use of HFECs in preventing postoperative complications by reducing the incidence of tissue coagulation [7].

Low-temperature plasma (LTP) at atmospheric pressure is available for use to control oozing bleeding by increasing blood coagulation activity and to prevent postoperative complications due to decreased tissue coagulation [10,11]. LTP treatment for hemostasis is generally assumed to be achieving by blood coagulation, like generation of clot formation by using the same mechanism as that in surgical hemostats for stimulating both platelets to aggregate and coagulation factors [12–14]. We recently demonstrated the plasma-induced aggregation of serum proteins, such as albumin and immunoglobulins [10], to generate membrane-like structures [10]. This suggested that LTP utilized much more abundant serum proteins (more than 70% of the total proteins) than coagulation factors (approximately 10% of the total proteins) for blood clot formation. Thus, our findings indicate the possibility that LTP treatment has the potential to induce whole-blood clot formation by mechanisms with or without platelet aggregation and coagulation factors.

In this study, we aimed to evaluate the effectiveness of LTP treatment involving erythrocytes to form clots based on the fact that plasma technology can convert red blood cells (RBCs), which make up approximately 35–50% of the blood volume [15], into an ingredient for blood coagulation. Erythrocytes isolated by using density gradient were suspended in phosphate-buffered saline (PBS) and subjected to a series of experiments for LTP treatments using two plasma devices; one is developed by Nagoya Univ. and the others by our institute and Nikon [10]. Data from histological and electron microscopic analyses of plasma-treated RBCs revealed that clot formation and hemolysis are essential processes for clot formation by LTP treatment.

2. Experimental details

2.1. Preparation of RBCs for plasma treatment

The use of human blood for LTP treatment was approved by the institutional ethics committee of the National Institute of Advanced Industrial Science and Technology (AIST) as (h2014-058). Seven milliliters of whole blood was isolated by using a blood collection tube with ethylenediamine tetraacetic acid (EDTA; Terumo, Tokyo, Japan). RBCs were isolated by using density-gradient centrifugation with Histopaque-1077 (Sigma-Aldrich, St. Louis, MO) according to the suppliers' manual, and the amount was adjusted to 2.0×10^9 /mL with Dulbecco's PBS (Wako Pure Chemical Industries, Ltd., Osaka, Japan) by using a hemocytometer (Sunlead Glass Corp., Ltd, Saitama, Japan).

2.2. LTP treatment at atmospheric pressure

Two different plasma instruments were used. One was BPC-HP1 (Nikon Co., Ltd. and AIST), which produced plasma using a dielectric barrier discharge technique. The plasma discharge was ignited using a sinusoidal peak-to-peak voltage of 6.0–9.0 kV at 62 kHz in frequency [11,16]. The other instrument used was PN-110/120TPG (NU Global Co., Ltd., Nagoya, Japan), which equipped a micro hollow discharge electrode (sinusoidal peak-to-peak voltage of 9.0 kV along a full waveform of 60 Hz) developed by Nagoya University [17]. The discharge tubes of BPC-HP1 and PN-110/120TPG have a single electrode and two electrodes, respectively. The inner diameter of the discharge tubes of both BPC-HP1 and PN-110/120TPG is 2 mm. For the plasma production using both devices, pure helium with a flow rate of 2 standard liters per minute was applied. The plasma flare comes out from the nozzle of the devices. The target material, at a volume of 1 mL, was placed in each well of a 24-well plate and placed at a distance of 10 mm. The plasma flares from both instruments were similar in visible appearance [10]. The surface temperature was maintained at room temperature in all the cases treated with the AIST instrument [11], whereas it was around 50 °C in some cases treated with the instrument developed by Nagoya University.

2.3. Light and electron microscopic analysis

Plasma-induced blood coagulations were subjected to the analysis with light and electron microscopic analysis. For light microscopic analysis, we performed according to standard protocols [18,19]. In brief, 3 μ m serial sections were prepared by analyzed by differential interference contrast microscopy (Axio Observer Z1 inverted microscope, Carl Zeiss, Oberkochen, Germany). For the scanning electron microscopy (SEM) and transmission electron microscopy (TEM), materials were fixed for 24 h in phosphate-buffered 2.5% glutaraldehyde (Wako Pure Chemical Industries, Ltd.). Postfixation for SEM and TEM was performed for 1 h in 1% osmium tetroxide and for 3 h in 2% osmium tetroxide in 0.1 M phosphate buffer (pH 7.4), respectively, in an ice bath. The specimens for SEM were dehydrated, mounted, and coated with gold in a sputter coater (JFC-1300 Auto Fine Coater, JEOL, Tokyo, Japan), and the samples were examined by using SEM (JSM-5600 LV SEM, JEOL). The specimens for TEM were embedded in epoxy resin. Ultrathin sections were cut and stained with uranyl acetate for 10 min, followed by a lead staining solution for 5 min, and examined by using TEM (JEM-1200 EX, JEOL) [10,20].

2.4. Evaluation of hemoglobin and residual numbers of RBCs after LTP treatment

LTP treatment was applied to a solution containing 2.0×10^9 RBCs and 1 mL PBS. The solution was recovered and placed into to 1.5-mL micro centrifuge tubes. After 10 min, centrifugation at 15,000g was performed at room temperature, and supernatants were recovered to identify the hemoglobin concentration by using a hemoglobin colorimetric assay kit (Cayman Chemical Company, Ann Arbor, MN) according the manufacturer's instructions. The reference standard curve was constructed from the reference hemoglobin concentration obtained by using the assay kit according to the supplier's manual.

2.5. Measurement of current through the targets contacting with the plasma flare

Fig. 1 shows the configuration of measurement system for the current through the targets contacting with the plasma flare. The

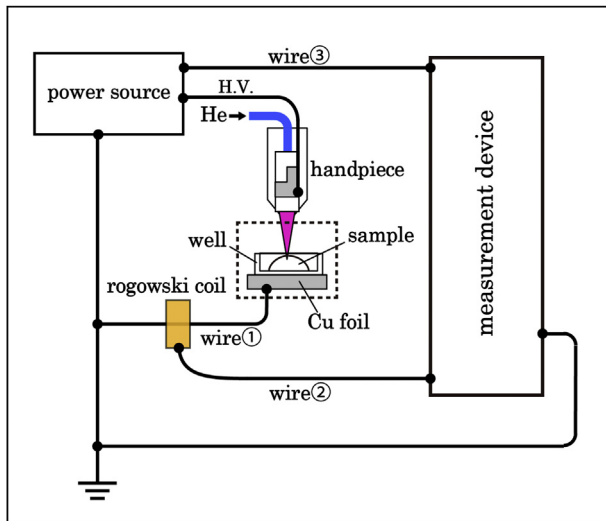


Fig. 1. The Configuration of measurement system for current through the targets contacting with the plasma flare. Stage for the samples is surrounded with dotted line. Surface of the stage is covered with copper foil connected by the conducting wire to the ground. Plasma flare contacts with a sample, which makes current flow toward the ground through the wire-1 passing through Rogowski coil. The induced current in the coil is detected through the wire-2. Results were displayed by the indicator on the side of the box and read out as analog data.

surface of the stage is covered with a copper foil connected to the ground. The area of the stage is 75×75 mm. Plasma flare contacts with the sample, the electrical current of which flows to the ground and through the Rogowski coil (CT-D5.0-BNC, Magnelab Inc., Longmont, Colorado) [21,22]. The voltage applied on the discharge tube was measured by using P6015A (TFF Corporation, Tokyo, Japan), while the measurement system detects the voltage of the discharge tube with wire 3 and the current through the sample with wire 2. The current through the sample were analyzed after the elimination of electrical noises including from the plasma discharge and adjusted by the results from the control experiments. The results were displayed on the measurement system and it can also provide data as analog signal.

3. Results and discussion

3.1. LTP treatment induced clots from whole blood

Earlier studies demonstrated that plasma treatment triggered clot formation in human whole blood through the activation of platelets and coagulation factors [12–14]. Meanwhile, we reported the appearance of eosinophilic membrane-like structure in mouse whole blood clots by LTP treatment using our developed instrument [11]. Consequently, first, we evaluated in this study the effectiveness of either BPC-HP1 or PN-110/120TPG to form human whole blood clots, as in mouse whole blood. Clot formation was observed within less than a second of contact with the plasma flare in human whole blood containing EDTA from healthy volunteer. However, neither clot formation nor evaporation that induces stable aggregation was observed after 5 min of helium gas flow treatment without plasma. In the control experiments, we confirmed that both types of plasma equipment could generate aggregation on the surface of 50-mg/mL bovine serum albumin solution after 10 s of the first contact with the plasma flare and that the surface temperature remained lower than 40°C – 50°C as in the control experiments (data not shown).

The generated clots were subjected to histological analysis

(Fig. 2a–c). Monotonous and membrane-like structures covered the clot formed by LTP treatment with BPC-HP1 (Fig. 2a). On the other hand, erythrocytes were compactly aggregated, maintaining the shape of the clot by LTP treatment with PN-110/120TPG (Fig. 2b). The histological appearance was essentially the same as that of the control collagen-induced clots (Fig. 2c), with neither the monotonous nor membrane-like structures. Electron microscopic analysis clearly confirmed the above-mentioned findings that the inability of deformed erythrocytes to fuse with each other was evident in the clots formed by LTP treatment with BPC-HP1, whereas the shape of the erythrocytes was maintained with LTP treatment with PN-110/120TPG and in the collagen-induced clots (Fig. 2d–f). Taken together, these results show that our newly developed BPC-HP1 produced whole-blood clots with a membrane-like structure without maintaining the shape of erythrocytes (Fig. 2a and d).

3.2. LTP treatment with BPC-HP1 formed RBC coagulation

To clarify the effect of LTP treatment on the shape of erythrocytes, RBCs were isolated by using density gradient to apply plasma treatment, because aggregated platelets and/or polymerized fibrin has been considered to alter the shape of RBCs in the bloodstream of patients with disseminated intravascular coagulation [23–25]. In the following LTP experiments, we used $2.0 \times 10^9/\text{mL}$ RBCs in PBS, in an amount equal to that in healthy humans.

LTP treatment with BPC-HP1 macroscopically formed stable clots. On the other hands, although PN-110/120TPG induced a condensed state of RBCs, this state disappeared after discontinuation of the plasma supply. Light microscopic analysis results showed that the shape of erythrocytes was altered after LTP treatment with BPC-HP1 to form clots with monotonous membrane-like structures (Fig. 3a). By contrast, LTP treatment with PN-110/120TPG formed packed erythrocytes, exclusively maintaining the shape of the erythrocytes (Fig. 3b). Moreover, electron microscopic analysis confirmed the above-mentioned findings that production of materials with monotonous texture was induced in clots formed by LTP treatment with BPC-HP1 (Fig. 3c). Among the packed erythrocytes induced by LTP treatment with PN-110/120TPG, densely packed erythrocytes with slight deformities were observed (Fig. 3d).

These results indicate that LTP treatment with BPC-HP1, but not PN-110/120TPG, could form clots in PBS containing $2.0 \times 10^9/\text{mL}$ RBCs through the essential step of hemolysis. Accordingly, we designated the clot from RBCs only as RBC clots to distinguish them from common clots that consist of aggregated platelets and fibrin with less hemolysis.

3.3. LTP treatment with BPC-HP1 effectively hemolyzed the erythrocyte membrane

As the shape of erythrocytes disappeared exclusively after LTP treatment with BPC-HP1 (Fig. 3a and c), we next evaluated the hemolysis effects of the LTP treatments with BPC-HP1 and PN-110/120TPG. Isolated erythrocytes were suspended in PBS at a concentration of 2×10^9 cells/mL and subjected to LTP treatment with either BPC-HP1 or PN-110/120TPG, or helium gas flow alone at 2 L/min.

The numbers of erythrocytes and hemoglobin concentration in 1 mL of PBS after each plasma treatment are shown in Fig. 4 and Table 1. Compared with that in helium gas treatment and LTP treatment with PN-110/120TPG, a significant decrease in the number of erythrocytes and a significant increase in hemoglobin concentration in PBS were observed after LTP treatment with BPC-HP1. The hemoglobin concentration in PBS corresponded to the

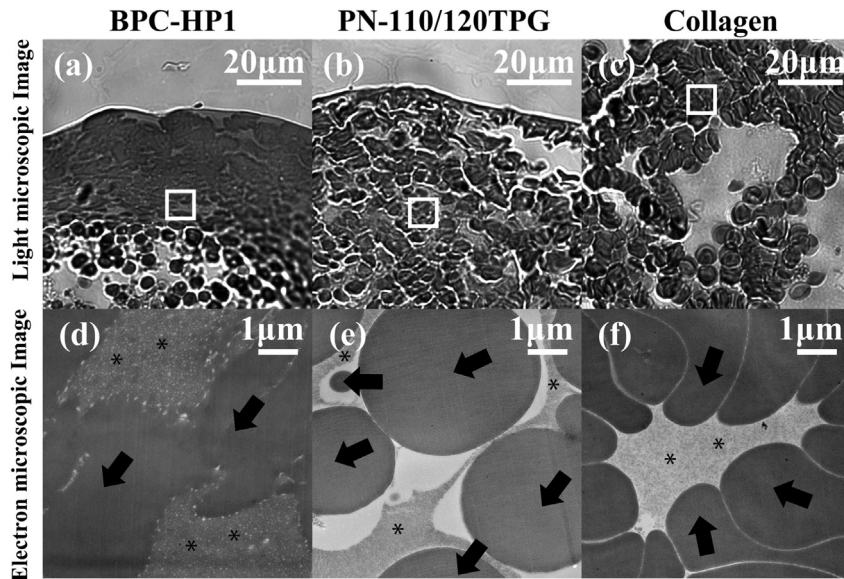


Fig. 2. Treatments with plasma flare produced by BPC-HP1 and PN-110/120TPG could form clots from whole blood but with differential morphology as determined histologically and ultrastructurally. (a and b) Light microscopic images of clots from whole blood treated with LTP with BPC-HP1 (a) and PN-110/120TPG (b). (c) Collagen-induced clots used as controls. (d and f) Electron microscopic images of clots from whole blood treated with LTP with BPC-HP1 (d) and PN-110/120TPG (f). (e) Collagen-induced clots used as controls. The arrows and asterisks indicate erythrocytes with coagulated plasma proteins, respectively.

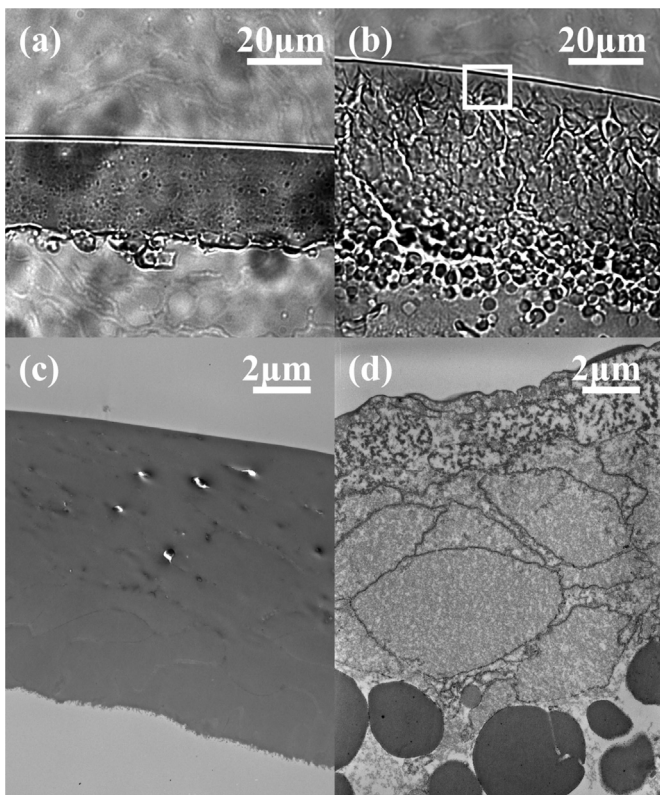


Fig. 3. LTP treatment with BPC-HP1 formed coagulation from RBCs. (a and b) Histological appearance of aggregated RBCs at 2.0×10^9 /mL in PBS followed by LTP treatment. (a) Histological appearance of formed monotonous membrane-like structures in clots induced by LTP treatment with BPC-HP1. (b) Densely packed erythrocytes in the clot induced by LTP treatment with PN-110/120TPG. (c) Electron microscopic image of the amorphous aggregates in the clots induced by LTP treatment with BPC-HP1. (d) Electron microscopic image of the aggregates of RBCs induced by LTP treatment with PN-110/120TPG.

hemoglobin concentration caused by the decreased number of erythrocytes after LTP treatments (Table 1). Although both PN-110/120TPG and BPC-HP1 could form aggregation in hemoglobin solution at 15 mg/mL in PBS (Fig. 4c), only LTP treatment with BPC-HP1 could form clots in PBS containing the isolated erythrocytes at 2×10^9 cells/mL. The amount of hemoglobin in PBS with the LTP treatment with BPC-HP1 was less than that estimated from the decreased number of erythrocytes, suggesting that the released hemoglobin from erythrocytes was included in the formed clot. Taken together, efficient hemolysis is essential to form the RBC clots that appeared after LTP treatment with BPC-HP1.

3.4. Hemolysis is correlated with current through the targets contacting with the plasma flare

Next, the current through the targets contacting with the plasma flare was measured in order to investigate the relation between the current and RBC clot formation. The performance-based parameters on the target is essential for the reproducibility of RBC clot formation by LTP treatment. To determine the electrical parameters from the LTP treatment with BPC-HP1, we performed real-time in-situ measurements by using our own equipment as shown in Fig. 1. The current measured with the Rogowski coil and the applied voltage on the plasma device were shown in Fig. 5a. The measured electrical current contains both displacement current and the current from the plasma discharge (from here we call LTP current). The displacement current is due to the capacitive component in the plasma system and the LTP current responsible for the plasma discharge has a spike-like shape. To estimate the current from the plasma discharge, the displacement current was estimated using the applied voltage as shown in Fig. 5b. The LTP current was obtained from the difference between the measured current and estimated from the time-averaged area Q_{LTP} as shown in Fig. 5c. We confirmed that the LTP current was constant at 0.80 ± 0.05 mA for up to 3 min and that the surface temperature of the treated area was lower than 50°C after LTP treatment.

In the next experiment, we examined the correlation between the hemolysis and the LTP current through samples using the LTP

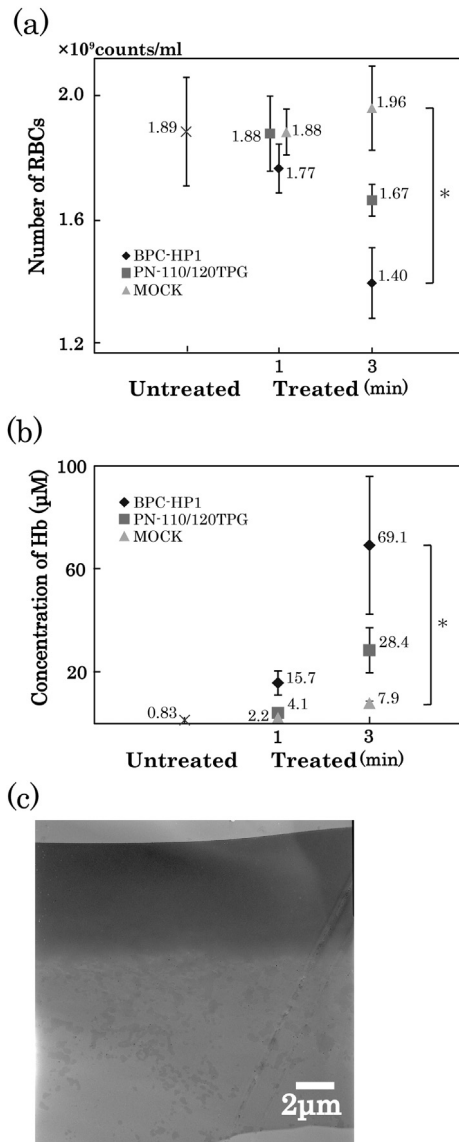


Fig. 4. Differential efficacy of hemolysis by the LTP treatment with BPC-HP1 and PN-110/120TPG. (a) The number of red blood cells and (b) the hemoglobin concentration in PBS after plasma treatment. (n = 3; p < 0.05; bars represent the mean values per microliter ± SD). Untreated and helium gas treatment (MOCK) are applied as control experiments. (c) An electron microscopic image of the aggregates in hemoglobin solution.

currents of 0.80 ± 0.05 , 0.60 ± 0.05 , 0.40 ± 0.05 , and 0.20 ± 0.05 mA. The results from each determined hemoglobin concentration in PBS indicated that efficient hemolysis occurred at the LTP current greater than 0.60 ± 0.05 mA as shown in Fig. 6. These results suggest that the LTP current through the targets contacting with the

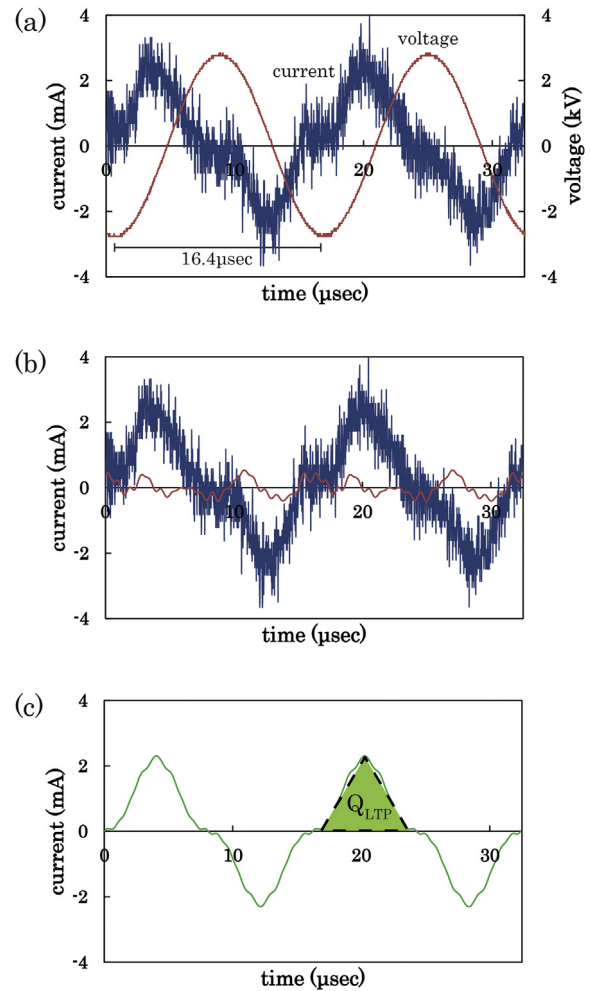


Fig. 5. Results of the measurement of the maximum output data of LTP with BPC-HP1. (a) Current introduced into the Rogowski coil and voltage in an electrode on a discharge tube. (b) Measured noise current and discharge tube voltage. (c) Graph showing the LTP current flowing through the targets in contact with the plasma flare.

plasma flare is feasible for use in the accuracy control of the efficacy for whole blood and RBC clot formation as a performance-based parameter of LTP.

4. Conclusion

The appearance of membrane-like structures in clots induced by LTP treatment was first reported by us, where we pointed out that erythrocytes might be a source for the formation of the membrane-like structure via hemolysis [11]. Whereas the aggregation of platelets and the activation of coagulation factors had been considered as main effects of plasma treatment in earlier studies

Table 1
Numbered of RBCs, Determined amounts of Hb, and Estimated amount of Hb (n = 3).

Per ml	Untreated	MOCK		BPC-HP1		PN-110/120TPG	
	–	1 min	3 min	1 min	3 min	1 min	3 min
Counted numbers of RBCs (number × 10 ⁸)	18.85	18.80	19.60	17.67	14.00	18.78	16.65
Decreased numbers of RBCs (number × 10 ⁸)	1.15	1.12	0.40	2.33	6.00	1.22	3.35
Determined amounts of Hb (mg)	0.02	0.04	0.13	0.25	1.11	0.07	0.46
Estimated amounts of Hb (mg)	3.57	3.47	1.24	7.53	18.6	3.82	10.4

MOCK:He gas treatment.

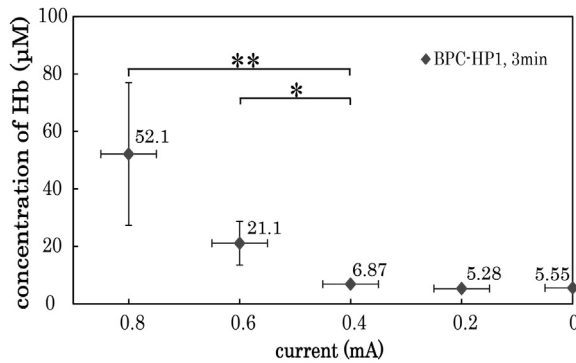


Fig. 6. Hemoglobin concentration in red blood cell solution increases along with increased plasma current. Hemoglobin concentration in PBS after plasma treatment. ($n = 3$; $p < 0.05$; bars represent mean values per microliter \pm SD).

[12–14], in this study, we demonstrated that the blood clot formation process in LTP treatment with BPC-HP1 differed from the natural blood clot formation process. Indeed, the alternate pathway has characteristic findings such as hemolysis and the appearance of a membrane-like structure derived from RBCs. Moreover, we demonstrated that the efficacy of hemolysis is correlated with the current through the targets contacting with the plasma flare on LTP treatment using BPC-HP1 (Fig. 6). The measurement of current through the targets in contact with the plasma flare is feasible for accuracy control of whole blood and RBC clot formation. However, further studies are needed to elucidate the underlying mechanism of hemolysis and hemoglobin coagulation by evaluating for the associated plasma parameters.

Through this study, we authenticated a different clot formation mechanism involving hemolysis of erythrocytes to coagulate from the already known clot formation process linked with plasma treatment. Based on our results, we named these clots “RBC clots”

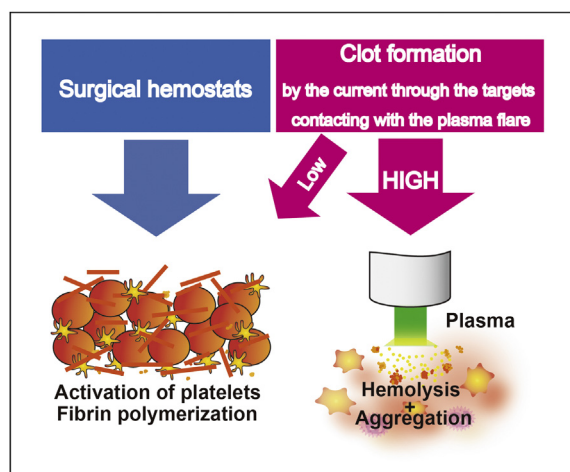


Fig. 7. Schematic illustration of plasma-induced blood coagulations. Plasma treatment induced clot formation coating the surface of wound without heat injury. In this study, we demonstrated that plasma can induce clot formation only from RBCs. The clot formed appears monotonous with membrane-like covering on light and electron microscopy. Meanwhile, LTP treatment has been considered to promote platelet aggregation and coagulation cascades to form whole-blood clots without hemolysis. Taken together, these results indicate that clot formations with plasma treatments can be classified into two types, namely classical (without hemolysis) and alternative (with hemolysis). It is noteworthy that increased plasma current correlated with hemolysis and the ability of serum proteins such as albumin to aggregate.

to describe a different mechanism of blood coagulation, which was included in the formed clots as membrane-like structure. A schematic illustration is shown in Fig. 7 to clarify the different mechanism. We propose here an alternate mechanism of plasma-induced blood coagulation and identified two types of blood clot formation by LTP treatment. An essential point is whether the clot formation was confined to the blood coagulation system or extended to other blood components with or without hemolysis.

The series of results from the histological and the electron microscopic analysis, and the measurement of plasma current revealed that the RBC clot formation occurred during hemolysis and protein coagulation. Indeed, PN-110/120TPG provided little hemolysis in PBS at 2×10^9 cells/mL, which was insufficient to form RBC clots. However, it could generate aggregation-like clots in PBS containing human hemoglobin at 15 mg/mL at 10 s after the first contact with the plasma flare, suggesting that hemolysis was a crucial step in RBC clot formation. Moreover, the effective hemolysis and RBCs disappeared with the decreased LTP current through the targets contacting with the plasma flare using BPC-HP1. These results suggest that any benefit afforded by improved plasma instrument availability following clot formation is outweighed by measurement of the current flow because it is closely linked with efficiency of hemolysis.

Acknowledgments

We thank Dr. Shin-shichi Hamada (Otsu Municipal Hospital) for the discussion on pathology. We thank Ms. Mika Hashimoto (Biotechnology Research Institute for Drug Discovery, AIST) and Ms. Sachie Matsubara (Laboratory for Electron Microscopy, Kyorin University School of Medicine) for their technical assistance. This work was supported by Grants-in-Aid for Scientific Research on Priority Areas (24108006, 10311440, and 15K08413 to Y. I.) from the Ministry of Education, Culture, Sports, Science and Technology of Japan, and in part by grants from the Advanced Research and Development Project “Molecular Probes for Detection of Biological Features on Cancer” from NEDO.

References

- [1] G.N. Box, H.J. Lee, J.B. Abraham, L.A. Deane, E.R. Elchico, C.A. Abdelshehid, R. Alipanah, M.B. Taylor, L. Andrade, R.A. Edwards, J.F. Borin, E.M. McDougall, R.V. Clayman, *J. Urol.* 181 (2009) 387–391.
- [2] P.A. Sutton, S. Awad, A.C. Perkins, D.N. Lobo, *Br. J. Surg.* 97 (2010) 428–433.
- [3] P.K. Tulikangas, T. Smith, T. Falcone, N. Boparai, M.D. Walters, *Fertil. Steril.* 75 (2001) 806–810.
- [4] F.J. Kim, M.F. Chammas Jr., E. Gewehr, M. Morihisa, F. Caldas, E. Hayacibara, M. Baptistussi, F. Meyer, A.C. Martins, *Surg. Endosc.* 22 (2008) 1464–1469.
- [5] B.J. O'Daly, E. Morris, G.P. Gavin, J.M. O'Byrne, G.B. McGuinness, *J. Mater. Process. Technol.* 200 (2008) 38–58.
- [6] K.E. Grundt, T. Straub, G. Farin, *Bailliere Best Pract. Res. Clin. Gastroenterol.* 13 (1999) 67–84.
- [7] N. Annabi, A. Tamayol, S.R. Shin, A.M. Ghaemmaghami, N.A. Peppas, A. Khademhosseini, *Nano Today* 9 (2014) 574–589.
- [8] G. Sankaranarayanan, R.R. Resapu, D.B. Jones, S. Schwaizberg, S. De, *Surg. Endosc.* 27 (2013) 3056–3072.
- [9] J.L. Mega, T. Simon, *Lancet* 386 (2015) 281–291.
- [10] S. Ikehara, H. Sakakita, K. Ishikawa, Y. Akimoto, Y. Yamaguchi, M. Yamagishi, J. Kim, M. Ueda, J. Ikeda, H. Nakanishi, N. Shimizu, M. Hori, Y. Ikehara, *Plasma Process. Polym.* 12 (2015) 1348–1353.
- [11] Y. Ikehara, H. Sakakita, N. Shimizu, S. Ikehara, H. Nakanishi, *J. Photopolym. Sci. Technol.* 26 (4) (2013) 555–557.
- [12] S.U. Kalghatgi, G. Fridman, M. Cooper, G. Nagaraj, M. Peddinghaus, M. Balasubramanian, V.N. Vasilets, A.F. Gutsol, A. Fridman, *IEEE Trans. Plasma Sci.* 35 (5) (2007) 1559–1566.
- [13] C.-Y. Chen, Hsin-Wen Fan, S.P. Kuo, J. Chang, T. Pedersen, T.J. Mills, C.-C. Huang, *IEEE Trans. Plasma Sci.* 37 (6) (2009) 993–999.
- [14] Gregory Fridman, Marie Peddinghaus, Manjula Balasubramanian, Halim Ayan, Alexander Fridman, Alexander Gutsol, A. Brooks, *Plasma Chem. Plasma Process.* 26 (4) (2006) 425–442.
- [15] V.T. Turitto, H.L. Goldsmith, in: J. Loscalzo, M. Creager, V. Dzau (Eds.), *Textbook of Vascular Medicine*, vol. 2, Little, Brown, New York, 1996, pp. 141–184.

- [16] H. Sakakita, Y. Ikehara, S. Kiyama, WO2012/005132 (2012).
- [17] Y. Nakai, T. Kumakura, K. Takeda, K. Ishikawa, H. Tanaka, H. Kano, H. Hashizume, H. Kondo, M. Sekine, M. Hori, Development of high density atmospheric pressure plasma source, in: The 2nd International Workshop on Plasma for Cancer Treatment, Nagoya, 2015.
- [18] Y. Ikehara, T. Niwa, L. Biao, S.K. Ikehara, N. Ohashi, T. Kobayashi, Y. Shimizu, N. Kojima, H. Nakanishi, *Cancer Res.* 66 (2006) 8740–8748.
- [19] Y. Ikehara, T. Sato, T. Niwa, S. Nakamura, M. Gotoh, S.K. Ikehara, K. Kiyohara, C. Aoki, T. Iwai, H. Nakanishi, J. Hirabayashi, M. Tatematsu, H. Narimatsu, *Glycobiology* 16 (2006) 777–785.
- [20] M. Ueyama, Y. Akimoto, T. Ichimiya, R. Ueda, H. Kawakami, T. Aigaki, S. Nishihara, *PLoS One* 5 (2010) e11557.
- [21] D.G. Pellinen, M.S. Di Capua, S.E. Sampayan, H. Gerbracht, M. Wang, *Rev. Sci. Instrum.* 51 (1980) 1535–1540.
- [22] D.A. Ward, J.L.T. Exon, *Eng. Sci. Educ. J.* 2 (1993).
- [23] J.R. O'Brien, *Lancet* 335 (1990) 711–713.
- [24] E. Regoeczi, M.L. Rubenberg, M.C. Brain, *Lancet* 1 (1967) 601–602.
- [25] J. Nowicka, M. Kotschy, K. Chwistecki, M. Jelen, *Haematol. Budap* 11 (1977) 359–364.